

Structure of Polymorphous Modifications of Double Sodium and Indium Phosphate

M. G. Zhizhin, V. A. Morozov,¹ A. P. Bobylev, A. M. Popov, F. M. Spiridonov,
L. N. Komissarova, and B. I. Lazoryak

Chemical Department, Moscow State University, 119899, Moscow, Russia

Received March 18, 1999; in revised form July 8, 1999; accepted September 15, 1999

Polymorphous modifications of β - and α - $\text{Na}_3\text{In}(\text{PO}_4)_2$ were synthesized and found to be related to the β - K_2SO_4 structure type. They crystallize in a monoclinic system (space groups $P2_1/c$ and $P2_1/m$, respectively), with unit cell parameters $a = 7.127(1) \text{ \AA}$, $b = 18.220(1) \text{ \AA}$, $c = 8.616(1) \text{ \AA}$, $\beta = 143.36(1)^\circ$ for β - $\text{Na}_3\text{In}(\text{PO}_4)_2$; and $a = 8.6335(1) \text{ \AA}$, $b = 5.4550(1) \text{ \AA}$, $c = 7.0482(1) \text{ \AA}$, $\beta = 90.295(1)^\circ$ for α - $\text{Na}_3\text{In}(\text{PO}_4)_2$. Their crystal structures were determined by Rietveld analysis [$R_{\text{wp}} = 7.72$, $R_1 = 3.02$ (β -); $R_{\text{wp}} = 6.59$, $R_1 = 3.06$ (α -)]. Indium cations occupy the X position while sodium cations occupy the X and Y positions of the β - K_2SO_4 -type structure. The PO_4^{3-} tetrahedron rotation leads to a decrease in the coordination number of the Y position.

© 2000 Academic Press

Key Words: phosphates; indium; sodium; X-ray diffraction; infrared spectroscopy; Rietveld.

1. INTRODUCTION

During the last decade a considerable amount of data on the synthesis, structure, and properties of $\text{Na}_3R(\text{AO}_4)_2$ ($A = \text{P, V, As}$; $R = \text{Y, Bi, Fe}$, rare earth elements) (1–8) have been accumulated. Most of these compounds crystallize in a β - K_2SO_4 -like structure (1–5), with eight varieties of crystal lattice for $\text{Na}_3R(\text{AO}_4)_2$ being distinguished (9). These distortions are realized depending on the size and nature of the chemical elements constituting the crystal lattice. The distortion increases in double phosphates $\text{Na}_3R(\text{PO}_4)_2$ depending on the decrease in R^{3+} cation radius. High-temperature modifications of $\text{Na}_3R(\text{PO}_4)_2$ compounds ($R = \text{Tm–Lu}$) crystallize in the Nasicon structure type (8).

Despite the great interest in Na_3AO_4 – RAO_4 systems, the complex compounds of indium and alkaline elements are poorly studied. The crystal structure of $\text{Na}_3\text{In}(\text{PO}_4)_2$ was studied while using the single crystal which was obtained by

the hydrothermal method [space group $P2_1/n$; $a = 5.141(1) \text{ \AA}$, $b = 18.197(2) \text{ \AA}$, $c = 7.136(1) \text{ \AA}$, $\beta = 92.355(2)^\circ$] (10). However, this structure is not associated with the definite structural type in which compounds of the $\text{Na}_3R(\text{AO}_4)_2$ type are crystallized.

The conditions of formation of $\text{Na}_3\text{In}(\text{PO}_4)_2$ polymorphous modification were investigated and their crystal structures were studied in this work.

2. EXPERIMENTAL

Synthesis

The low-temperature β modification of sodium and indium double phosphate was obtained by hydrothermal synthesis from starting reagents In_2O_3 , $\text{Na}_2\text{HPO}_4 \cdot 2\text{H}_2\text{O}$, $\text{NaH}_2\text{PO}_4 \cdot 2\text{H}_2\text{O}$ (Na:P and Na:In starting molar ratios 1.667–1.778 and 7.5, respectively), and H_2O . This compound was synthesized at $T = 473 \text{ K}$ and $P = 20 \text{ bar}$ for 12–24 h. These conditions of hydrothermal synthesis differ much from the conditions reported by Lii (10) ($T = 600^\circ\text{C}$ and $P = 2400 \text{ MPa}$ for 40 h, Na:P molar ratio = 1.667).

Formation of sodium and indium phosphate as the white sediment was observed after 12 h. The product was filtered off, washed with water, rinsed with ethanol, dried at $T = 333 \text{ K}$, and examined by powder X-ray diffraction.

α - $\text{Na}_3\text{In}(\text{PO}_4)_2$ was prepared by sintering a stoichiometric ratio of In_2O_3 , $(\text{NH}_4)_2\text{HPO}_4$, and Na_2CO_3 at 1123 K for 120 h in air. The end of the reaction was tested by X-ray method [diffractometer Dron-3M ($\text{CoK}\alpha$ radiation, $\lambda = 1.79021 \text{ \AA}$, Fe filter)].

X-Ray Powder Diffraction

Powder diffraction data for indexing of the X-ray patterns and structure refinement of $\text{Na}_3\text{In}(\text{PO}_4)_2$ polymorphous modifications were obtained at room temperature in Bragg–Brentano geometry using a Siemens D500 powder diffractometer equipped with a primary SiO_2 monochromator ($\text{CuK}\alpha_1$ radiation, $\lambda = 1.5406 \text{ \AA}$) and a

¹ To whom correspondence should be addressed. Fax: (095) 938 24 57. E-mail: morozov@tech.chem.msu.ru.

position-sensitive detector (Braun). The data were collected over the range 8–110° (2θ) with a step of 0.02°; effective counting time was ca. 30 min per step.

The comparison of reflex positions in the X-ray pattern of the sample obtained by the hydrothermal method and the theoretical X-ray pattern calculated on the basis of atomic coordinates in the $\text{Na}_3\text{In}(\text{PO}_4)_2$ structure (10) indicates their identity. Indexing of the $\beta\text{-Na}_3\text{In}(\text{PO}_4)_2$ X-ray pattern was carried out in a monoclinic system [space group $P2_1/c$, $a = 7.129(1)$ Å, $b = 18.232(2)$ Å, $c = 8.617(1)$ Å, $\beta = 143.35(1)^\circ$; or space group $P2_1/n$; $a = 5.148$ Å, $b = 18.232$ Å, $c = 7.129$ Å, $\beta = 92.40$]. The choice of the space group ($P2_1/c$) was determined by its standard format in contrast to the space group $P2_1/n$ referred in (10).

The analysis of the reflex positions in the X-ray pattern of the sample obtained by the solid-state reaction has shown that $\alpha\text{-Na}_3\text{In}(\text{PO}_4)_2$ is isotypic with $\text{K}_3\text{Nd}(\text{PO}_4)_2$ (11). Indexing of the X-ray pattern of $\alpha\text{-Na}_3\text{In}(\text{PO}_4)_2$ was carried out in a monoclinic system [space group $P2_1/m$, $a = 8.640(1)$ Å, $b = 5.461(1)$ Å, $c = 7.056(1)$ Å, $\beta = 90.32(1)^\circ$].

Thermal Analyses

Thermogravimetric analyses (DTA, TG, DTG) of sodium and indium double phosphate polymorphous modifications were performed using the derivatograph OD-103. Samples were heated from 300 to 1273 K at 10 K/min in air and then cooled.

From the thermal analyses it was found that the $\beta \rightarrow \alpha$ transition occurs irreversibly at 973 K. This transition was observed only for samples synthesized by the hydrothermal method. Such an effect was not observed for samples synthesized by the solid-state reaction. The $\alpha\text{-Na}_3\text{In}(\text{PO}_4)_2$ phase is stable up to 1183 K. Above this temperature α -

TABLE 1
IR Spectra of β - and $\alpha\text{-Na}_3\text{In}(\text{PO}_4)_2$ in the PO_4^{3-} Vibrations Region

Assignment	$\beta\text{-Na}_3\text{In}(\text{PO}_4)_2$	$\alpha\text{-Na}_3\text{In}(\text{PO}_4)_2$
ν_{2E}	445 w; 463 w ^a	448 m; 454 sh
ν_{4F2}	558 m; 571 m; 582 m; 589 m; 607 w; 622 m	553 w; 578 s; 623 s
ν_{1A}	993 sh, w	989 sh
ν_{3F2}	945 m; 961 m; 972 s; 977 sh; 1011 vs; 1028 s; 1042 sh; 1115 m; 1127 m; 1145 m; 1166 sh	953 s; 1063 s; 1130 s
PO_4^{3-} -site symmetry	C_1	C_1
PO_4^{3-} factor group	C_{2h}	C_{2h}

^aw, weak; m, medium; s, strong; vs, very strong; sh, shoulder.

$\text{Na}_3\text{In}(\text{PO}_4)_2$ decomposes into sodium orthophosphate and a new phase with containing an considerable amount of indium crystallizing into the Nasicon-like structure (8, 12).

IR Spectroscopy

IR spectra were recorded on the Nicolet Magna-750 Fourier spectrometer in the range 400–4000 cm^{-1} .

The IR spectra of $\text{Na}_3\text{In}(\text{PO}_4)_2$ polymorphous modifications are given in Fig. 1. Analysis of spectra for β - and $\alpha\text{-Na}_3\text{In}(\text{PO}_4)_2$ was carried out in the area of PO_4^{3-} group oscillations. Splitting of degenerated oscillation bands (Table 1) and the presence of two unequivalent PO_4^{3-} groups in an elementary cell were revealed. The symmetry of PO_4^{3-} groups increases during the transition from the low-temperature β -modification to the high-temperature α modification of $\text{Na}_3\text{In}(\text{PO}_4)_2$.

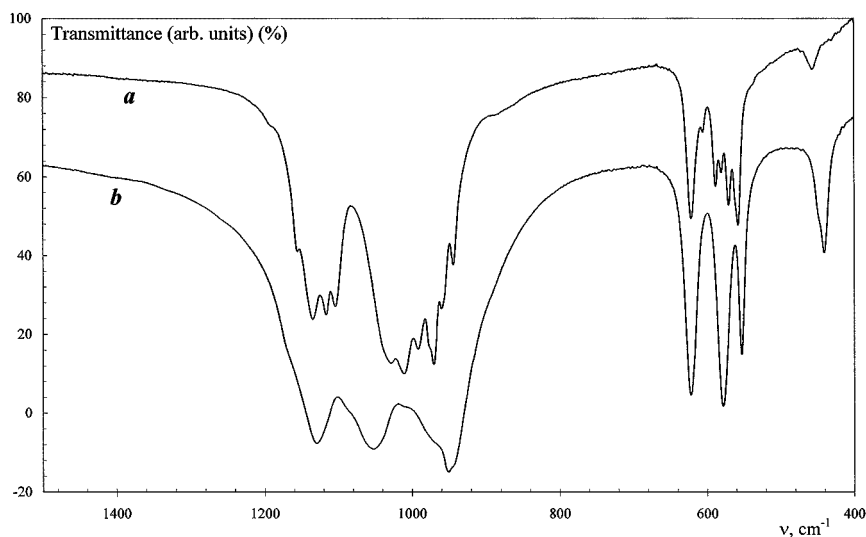


FIG. 1. IR spectra of $\beta\text{-Na}_3\text{In}(\text{PO}_4)_2$ (a) and $\alpha\text{-Na}_3\text{In}(\text{PO}_4)_2$ (b).

TABLE 2
Crystallographic Data, Recording Conditions, and Refinement
Results for β - and α - $\text{Na}_3\text{In}(\text{PO}_4)_2$

	β -modification	α -modification
T (K)	297	297
Space group	$P2_1/c^a$	$P2_1/m$
Z	4	2
2θ range ($^\circ$)	8–110	10–110
Step scan increment	0.02	0.02
I_{\max}	43,212	47,204
Unit cell parameters		
a (\AA)	7.127(1)	8.6335(1)
b (\AA)	18.220(1)	5.4550(1)
c (\AA)	8.616(1)	7.0482(1)
β ($^\circ$)	143.36(1)	90.295(1)
V (\AA^3)	667.7(1)	331.9(1)
Number of reflections	847	468
Variables		
Structural	53	35
Others	19	19
Reliability factors ^b		
$R_{\text{WP}}, R_{\text{P}}$	7.72, 5.65	6.59, 5.05
$R_{\text{I}}, R_{\text{F}}$	3.02, 1.60	3.06, 1.75

^a For space group $P2_1/n$: $a = 5.146 \text{ \AA}$, $b = 18.220 \text{ \AA}$, $c = 7.127 \text{ \AA}$, $\beta = 92.378$.

^b $R_{\text{WP}} = \{(\sum_w [y_i(\text{obs.}) - y_i(\text{calc.})]^2 / (\sum_w [y_i(\text{obs.})]^2))^{1/2}$,
 $R_{\text{P}} = (\sum [y_i(\text{obs.}) - y_i(\text{calc.})] / (\sum y_i(\text{obs.})))$,
 $R_{\text{I}} = (\sum |I(\text{obs.}) - I(\text{calc.})| / (\sum I(\text{obs.})))$,
 $R_{\text{F}} = (\sum [|I(\text{obs.})|^{1/2} - |I(\text{calc.})|^{1/2}] / (\sum [I(\text{obs.})]^{1/2}))$.

Structure Determination

The β - $\text{Na}_3\text{In}(\text{PO}_4)_2$ structure was refined for the following reasons: (1) the conditions of our hydrothermal synthesis differed considerably from the conditions used earlier (10);

(2) the single crystal can inadequately represent a powder-like substance. Atomic coordinates of $\text{Na}_3\text{In}(\text{PO}_4)_2$ (10) and $\text{K}_3\text{Nd}(\text{PO}_4)_2$ (11) structures were used as initial positional parameters for the refinement of crystal structure, which was carried out by the Rietveld method (13) and with the Rietan-94 program (14, 15). Scattering factors for Na^+ , In^{3+} , P, and O^- were used. The background was refined with a fifth-order polynomial. The peak profile was refined using a modified Pseudo-Voigt function. The occupancy factor for indium and all sodium positions was allowed to refine but did not deviate significantly from full occupation.

After the last refinement there was good agreement between the observed and calculated patterns and reasonable values of isotropic temperature parameters for all atoms. Final plots of the observed electron density maps did not show residual peaks. The electron density of different electron density maps $[\Delta\rho_{\text{exp.}}(xyz)]$ was within $\pm 0.7\bar{e} \text{ \AA}^{-3}$. The electron density maps were calculated using the GSAS program (16). The details of data collection and refinement are given in Table 2. Figures 2 and 3 display the Rietveld plots showing the good agreement between observed and, calculated patterns. The final atomic parameters are listed in Table 3. Table 4 presents important interatomic distances.

3. RESULTS AND DISCUSSION

Comparison of the $\text{Na}_3\text{In}(\text{PO}_4)_2$ polymorphous modification structures with those of $\text{Na}_3\text{Er}(\text{VO}_4)_2$ (3) and $\text{K}_3\text{Nd}(\text{PO}_4)_2$, investigated earlier (11) (Fig. 4) reveals that β and α modifications of double sodium and indium phosphate crystallize in a β - K_2SO_4 -like structure. The β - $\text{Na}_3\text{In}(\text{PO}_4)_2$ structure differs from that of $\text{Na}_3\text{Er}(\text{VO}_4)_2$ in

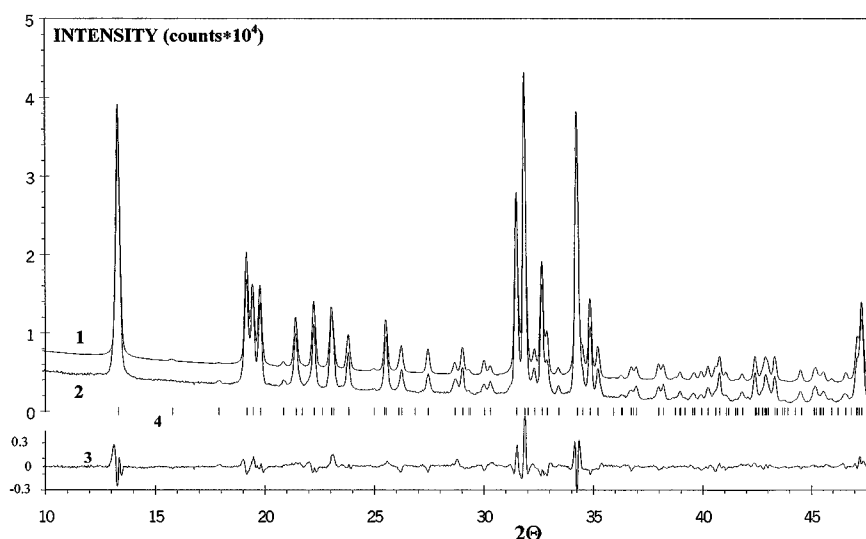


FIG. 2. Portion of the Rietveld refinement profiles for β - $\text{Na}_3\text{In}(\text{PO}_4)_2$: (1) calculated, (2) observed, and (3) difference X-ray powder diffraction patterns; (4) Bragg reflections. The calculated pattern is shifted to 2500 counts from the observed pattern.

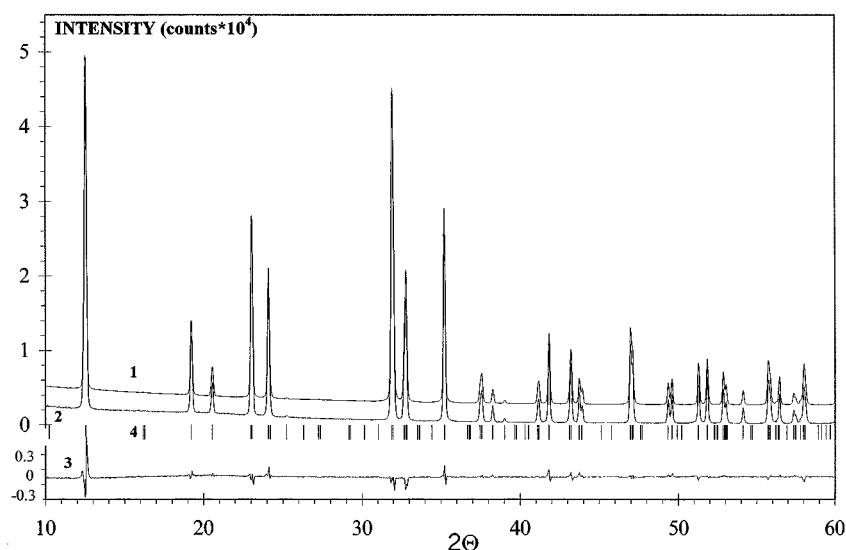


FIG. 3. Portion of the Rietveld refinement profiles for α - $\text{Na}_3\text{In}(\text{PO}_4)_2$; (1) calculated, (2) observed, and (3) difference X-ray powder diffraction patterns; (4) Bragg reflections. The calculated pattern is shifted to 2500 counts from the observed pattern.

the double b parameter. The basic frame of $\text{K}_3\text{Nd}(\text{PO}_4)_2$ in α - $\text{Na}_3\text{In}(\text{PO}_4)_2$ remains the same despite the PO_4^{3-} tetrahedron rotation.

The $\text{Y}^{[4+6]}\text{O}_{10}$ polyhedron in the β - K_2SO_4 -like structure is formed by 10 atoms of oxygen: four of them are closer to the Y position than the other six (edges of three tetrahedra). The nearest six oxygen atoms (one out of each tetrahedron) and three remote apical oxygen atoms participate in the formation of $\text{X}^{[6+3]}\text{O}_9$ polyhedra. In double phosphates of $\text{Na}_3\text{R}(\text{PO}_4)_2$ (R is a rare earth element) (1–4) sodium and rare earth element cations systematically occupy the X position. The Y position is occupied by sodium cations. Distortion of the ideal crystal lattice of the β - K_2SO_4 type is caused by PO_4^{3-} tetrahedron rotation and depends on a set of elements. This phenomenon leads to the change in coordination polyhedra (Na, 6–7; R, 6–8) (17).

In β - and α - $\text{Na}_3\text{In}(\text{PO}_4)_2$ structures the X position is occupied by sodium and indium cations, similar to well-known double phosphates of $\text{Na}_3\text{R}(\text{PO}_4)_2$ ($R = \text{Bi}$, rare earth elements) with β - K_2SO_4 -type structure. Only six oxygen atoms, owing to rotation of PO_4^{3-} tetrahedra and removal of apical oxygen atoms, form the coordination polyhedron of the X position. The InO_6 octahedron is slightly deformed with In–O distances equal to 2.10–2.22 Å (for β modification) and 2.13–2.18 Å (for α modification). The $\text{Na}(\text{1})\text{O}_6$ octahedron is deformed much more strongly [distance Na(1)–O is equal to 2.04–2.79 Å (for β modification) and 2.25–2.54 Å (for α modification)]. The Y position in β - and α - $\text{Na}_3\text{In}(\text{PO}_4)_2$ structures is occupied by sodium cations. The PO_4^{3-} tetrahedron rotation leads to a decrease in the coordination number of sodium cations in Y positions to 8–9 (Table 4, Fig. 5).

The unit cell parameters of β - $\text{Na}_3\text{In}(\text{PO}_4)_2$ refined by powder diffraction data differ little from those reported by Lii (10). However, a significant difference in the interatomic distances is observed both in Na and In polyhedra and in PO_4^{3-} tetrahedra (Table 4).

During the structural transition from β - to α - $\text{Na}_3(\text{PO}_4)_2$, the symmetry of NaO_n polyhedra increases (Fig. 5). However, the same distances in the NaO_n polyhedra are shorter than the predicted values [$r_{\text{VI}}(\text{Na}^+) + r(\text{O}^{2-}) = 2.40$ Å and $r_{\text{VIII}}(\text{Na}^+) + r(\text{O}^{2-}) = 2.56$ Å] (Table 4), which is probably, the reason for the irreversible transition $\beta \rightarrow \alpha$.

In the structure β - $\text{Na}_3(\text{PO}_4)_2$ all NaO_n polyhedra are connected to each other: $\text{Na}(\text{1})\text{O}_6$ and $\text{Na}(\text{3})\text{O}_8$ via the edge O(12)–O(22), $\text{Na}(\text{2})\text{O}_8$ and $\text{Na}(\text{3})\text{O}_8$ via the edge O(12)–O(24), $\text{Na}(\text{1})\text{O}_6$ and $\text{Na}(\text{2})\text{O}_8$ via the facet O(11)–O(12)–O(22) (Fig. 5). The minimum distances Na–O in the structure β - $\text{Na}_3(\text{PO}_4)_2$ are observed for oxygen atoms O(12) and O(24), common for two or three NaO_n polyhedra (Table 4). To relieve tension along the edge O(12)–O(24), the structure tries to turn polyhedra $\text{Na}(\text{2})\text{O}_8$ and $\text{Na}(\text{3})\text{O}_8$. This leads to the irreversible transition $\beta \rightarrow \alpha$. In the structure α - $\text{Na}_3(\text{PO}_4)_2$, polyhedra $\text{Na}(\text{2})\text{O}_8$ and $\text{Na}(\text{3})\text{O}_8$ have no contiguous point. They are connected by common edges O(12)–O(22) and O(13)–O(23) only with $\text{Na}(\text{1})\text{O}_6$ (Fig. 5).

On the basis of interatomic distance analysis in structures of polymorphous modifications of double sodium and indium phosphates it is possible to make a conclusion about the existence of two types of PO_4^{3-} tetrahedra in the structure (Table 4). This fact is supported by the IR spectroscopy data (Table 1). All bands of degenerate oscillations of the PO_4^{3-} group are split into several components. IR spectra correspond to the site symmetry of PO_4^{3-} groups and to the

TABLE 3
Atomic Coordinates and Thermal Parameters for $\text{Na}_3\text{In}(\text{PO}_4)_2$

Atom		β modification	α modification
In	x	0.796(1)	0.25
	y	0.872(1)	0.25
	z	0.784(1)	0.00
Na(1)	B_{iso}	0.83(6)	0.39(2)
	x	0.295(2)	0.251(3)
	y	0.8751(5)	0.25
	z	0.781(2)	0.502(2)
Na(2)	B_{iso}	1.1(1)	1.40(8)
	x	0.618(2)	0.559(2)
	y	0.8037(5)	0.25
	z	0.309(2)	0.286(2)
Na(3)	B_{iso}	1.1(1)	1.29(6)
	x	0.958(2)	0.939(2)
	y	0.9473(5)	0.25
	z	0.249(2)	0.714(2)
P(1)	B_{iso}	1.1(1)	1.29(6)
	x	0.077(2)	0.596(1)
	y	0.7121(4)	0.25
	z	0.800(1)	0.778(2)
P(2)	B_{iso}	0.3(1)	0.8(2)
	x	0.508(2)	0.903(1)
	y	0.0353(4)	0.25
	z	0.726(1)	0.221(2)
O(11)	B_{iso}	0.3(1)	0.8(2)
	x	0.057(3)	0.498(2)
	y	0.8002(9)	0.25
	z	0.813(3)	0.963(2)
O(12)	B_{iso}	0.9(1)	0.48(5)
	x	0.038(3)	0.509(2)
	y	0.6696(7)	0.25
	z	0.934(3)	0.583(2)
O(13)	B_{iso}	0.9(1)	0.48(5)
	x	0.829(4)	0.301(1)
	y	0.6916(8)	50.06(2)
	z	0.510(3)	0.222(2)
O(14)	B_{iso}	0.9(1)	0.48(5)
	x	0.402(3)	—
	y	0.6955(7)	—
	z	0.953(3)	—
O(21)	B_{iso}	0.9(1)	0.48(5)
	x	0.252(4)	0.007(2)
	y	0.0664(8)	0.25
	z	0.463(3)	0.051(2)
O(22)	B_{iso}	0.9(1)	0.48(5)
	x	0.519(3)	0.209(1)
	y	0.9517(9)	0.531(2)
	z	0.738(3)	0.785(2)
O(23)	B_{iso}	0.9(1)	0.48(5)
	x	0.821(3)	0.006(2)
	y	0.0704(7)	0.25
	z	0.867(3)	0.391(2)
O(24)	B_{iso}	0.9(1)	0.48(5)
	x	0.452(3)	—
	y	0.0598(7)	—
	z	0.854(3)	—

expected modes for the C_{2h} factor group. Even though α - and β - $\text{Na}_3\text{In}(\text{PO}_4)_2$ have the same site symmetry of PO_4^{3-} groups, different numbers of bands are observed in the IR spectra. The increase in the number of bands in the IR spectra of β - $\text{Na}_3\text{In}(\text{PO}_4)_2$ may be related to the following reasons: there is a greater difference in the P–O bond

TABLE 4
Important Interatomic Distances (Å) for $\text{Na}_3\text{In}(\text{PO}_4)_2$

Distance	β modification	(10)	Distance	α modification
In–O(11)	2.12(1)	2.174	In–O(11)	2.16(2)
–O(13)	2.11(2)	2.152	–O(13) × 2	2.14(1)
–O(14)	2.16(1)	2.146	–O(21)	2.13(2)
–O(21)	2.18(1)	2.139	–O(22) × 2	2.18(1)
–O(22)	2.22(1)	2.168		
–O(23)	2.10(1)	2.149		
⟨In–O⟩	2.15	2.155	⟨In–O⟩	2.16
Na(1)–O(11)	2.36(2)	2.344	Na(1)–O(12)	2.30(3)
–O(12)	2.04(1)	2.225	–O(13) × 2	2.45(2)
–O(13)	2.79(2)	2.774	–O(22) × 2	2.54(2)
–O(21)	2.76(2)	2.749	–O(23)	2.25(3)
–O(22)	2.36(2)	2.423		
–O(24)	2.33(1)	2.242		
⟨Na(1)–O⟩	2.44	2.459	⟨Na(1)–O⟩	2.42
Na(2)–O(11)	2.61(1)	2.718	Na(2)–O(11)	2.34(2)
–O(11)′	2.62(2)	2.485	–O(12)	2.14(2)
–O(12)	2.28(2)	2.339	–O(12)′ × 2	2.939(7)
–O(13)	2.29(1)	2.323	–O(13) × 2	2.67(2)
–O(14)	2.64(2)	2.821	–O(22) × 2	2.39(2)
–O(14)′	2.84(2)	2.567		
–O(21)	2.72(1)	2.773		
–O(24)	2.70(1)	2.638		
⟨Na(2)–O⟩	2.59	2.583	⟨Na(2)–O⟩	2.56
–O(23)	3.12(2)	3.086		
Na(3)–O(12)	2.44(1)	2.477	Na(3)–O(13) × 2	2.51(2)
–O(13)	2.91(2)	2.963	–O(21)	2.44(2)
–O(21)	2.51(1)	2.394	–O(22) × 2	2.83(2)
–O(22)	2.59(2)	2.585	–O(23)	2.35(2)
–O(22)′	2.66(2)	2.695	–O(23)′ × 2	2.865(6)
–O(23)	2.47(1)	2.458		
–O(24)	2.28(1)	2.336		
–O(24)′	3.02(2)	2.881		
⟨Na(3)–O⟩	2.61	2.599	⟨Na(3)–O⟩	2.65
P(1)–O(11)	1.62(2)	1.562	P(1)–O(11)	1.56(2)
–O(12)	1.55(1)	1.504	–O(12)	1.57(2)
–O(13)	1.59(1)	1.556	–O(13) × 2	1.60(1)
–O(14)	1.51(1)	1.547		
⟨P(1)–O⟩	1.57	1.542	⟨P(1)–O⟩	1.58
P(2)–O(21)	1.47(2)	1.564	P(2)–O(21)	1.50(2)
–O(22)	1.53(2)	1.553	–O(22) × 2	1.54(1)
–O(23)	1.59(1)	1.536	–O(23)	1.48(2)
–O(24)	1.50(1)	1.504		
⟨P(2)–O⟩	1.52	1.539	⟨P(2)–O⟩	1.52

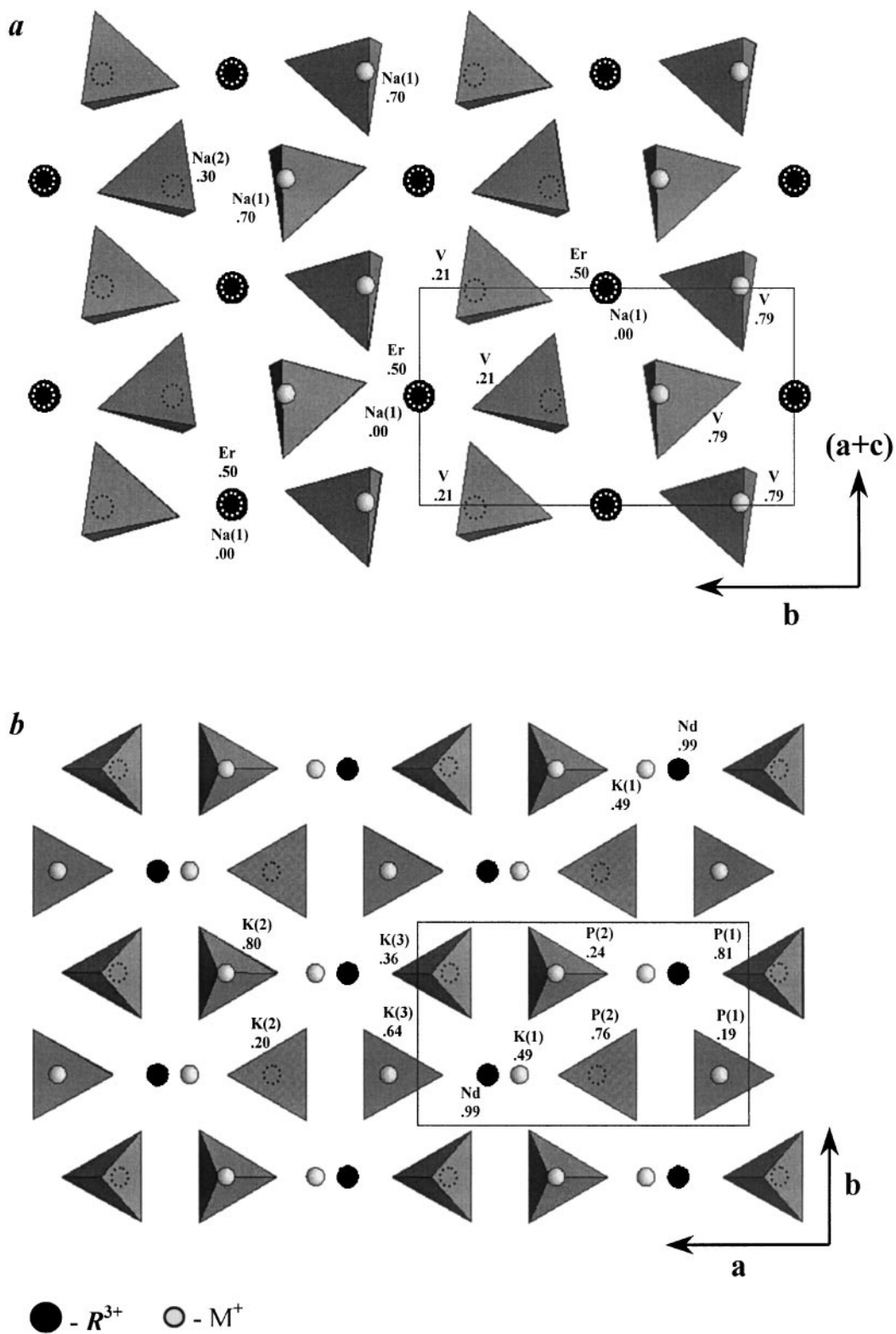


FIG. 4. Projection of $\text{Na}_3\text{Er}(\text{VO}_4)_2$ (a), $\text{K}_3\text{Nd}(\text{PO}_4)_2$ (b) $\beta\text{-Na}_3\text{In}(\text{PO}_4)_2$ (c), and $\alpha\text{-Na}_3\text{In}(\text{PO}_4)_2$ (d) structures. ●, - R^{3+} ; ○, - M^+ .

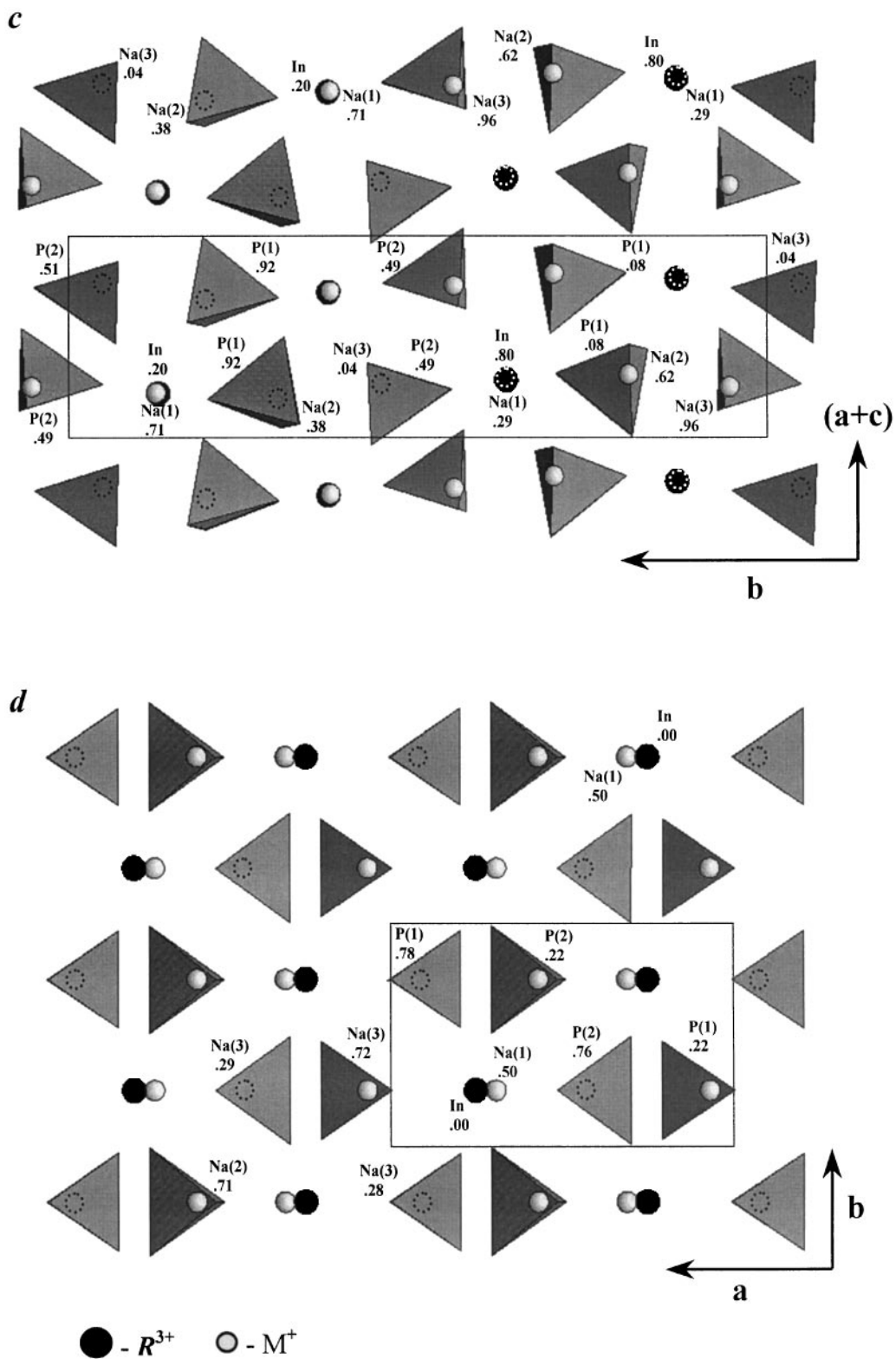


FIGURE 4—Continued

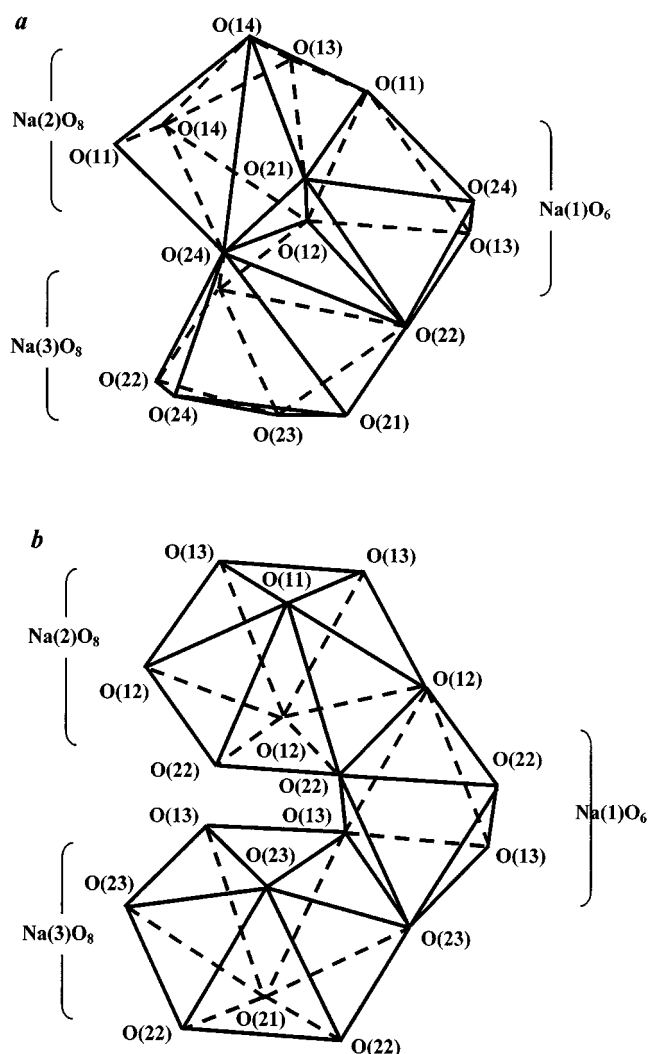


FIG. 5. Polyhedra of sodium cations in structures $\beta\text{-Na}_3\text{In}(\text{PO}_4)_2$ (a) and $\alpha\text{-Na}_3\text{In}(\text{PO}_4)_2$ (b).

lengths in the PO_4^{3-} tetrahedra and a decrease in distances between PO_4^{3-} in this structure. The latter factor leads to an increase in the resonance interaction between PO_4^{3-} anions.

β - and $\alpha\text{-Na}_3\text{In}(\text{PO}_4)_2$ have been defined as having the $\beta\text{-K}_2\text{SO}_4$ structure type. They differ from each other by the degree of structure distortion, which is also characteristic of low-temperature $\text{Na}_3R(\text{PO}_4)_2$ modifications ($R = \text{La-Lu}$) (1-4). High-temperature modifications of $\text{Na}_3R(\text{PO}_4)_2$ ($R = \text{Tm-Lu}$) crystallize in the Nasicon structure type.

Suffice it to say that the Nasicon-like phase is a product of $\alpha\text{-Na}_3\text{In}(\text{PO}_4)_2$ disintegration, which was discovered after heating $\alpha\text{-Na}_3\text{In}(\text{PO}_4)_2$ at temperatures higher than 1183 K.

The author (17) proposed regarding the vicinity of cation radii in YO_{10} and XO_9 polyhedra as criteria for stability of the $\beta\text{-K}_2\text{SO}_4$ -like structure. However, the difference in cation radii (Δr) of sodium ($r_{\text{VIII}}(\text{Na}^+) = 1.16 \text{ \AA}$ (18)) and indium [$r_{\text{VI}}(\text{In}^{3+}) = 0.79 \text{ \AA}$ (18)] in the Y position is greater (0.37 \AA) than the corresponding values for $\text{Na}_3R(\text{PO}_4)_2$ ($R = \text{Nd}^{3+}, \text{Yb}^{3+}$): 0.165 and 0.302 \AA , respectively [$r_{\text{VI}}(\text{Nd}^{3+}) = 0.995 \text{ \AA}$; $r_{\text{VI}}(\text{Yb}^{3+}) = 0.858 \text{ \AA}$]. It can be assumed that electronic structure influences the stability of $\beta\text{-K}_2\text{SO}_4$ -type or Nasicon-like structures of $\text{Na}_3R(\text{PO}_4)_2$ compounds to the same extent as the size of the R^{3+} cation.

ACKNOWLEDGMENTS

This work was supported by the Russian Fundamental Research Foundation (No. 98-03-32-688) and ICDD Grant-in-Aid 93-08.

REFERENCES

1. M. Vlasse, R. Salmon, and C. Parent, *Inorg. Chem.* **15**, 1440 (1976).
2. R. Salmon, C. Parent, M. Vlasse, and G. Le Flem, *Mater. Res. Bull.* **13**, 439 (1978).
3. R. Salmon, C. Parent, G. Le Flem, and M. Vlasse, *Acta Crystallogr. Sect. B* **32**, 2799 (1976).
4. C. Parent, J. Fava, R. Salmon, M. Vlasse, G. Le Flem, P. Hagenmuller, E. Antic-Fidancev, M. Lemaitre-Blaise, and P. Caro, *Nouv. J. Chim.* **3**, 523 (1979).
5. B. I. Lazoryak, V. N. Golubev, N. L. Kishkin, A. A. Shviryaev, and R. G. Aziev, *Zh. Neorg. Khim. (Russ.)* **32**, 753 (1987).
6. B. I. Lazoryak, S. Yu. Oralkov, and R. G. Aziev, *Zh. Neorg. Khim. (Russ.)* **33**, 453 (1988).
7. G. V. Zimina, I. N. Smirnova, S. I. Kudryashova, F. M. Spiridonov, and I. F. Poletaev, *Zh. Neorg. Khim. (Russ.)* **35**, 2134 (1990).
8. R. Salmon, C. Parent, and G. Le Flem, *Mater. Res. Bull.* **14**, 85 (1979).
9. M. Vlasse, C. Parent, G. Le Flem, and P. Hagenmuller, *J. Solid State Chem.* **35**, 318 (1980).
10. K.-H. Lii, *Eur. J. Solid State Inorg. Chem.* **33**, 519 (1996).
11. H. Y-P. Hong, and S. R. Chinn, *Mater. Res. Bull.* **11**, 421 (1976).
12. Powder Diffraction File, Card 47-77, JCPDS; International Center for Diffraction Data, 1601 Park Lane, Swarthmore, PA 19081.
13. H. M. Rietveld, *Acta Crystallogr.* **22**, 151 (1967).
14. F. Izumi, in "The Rietveld Method" (R. A. Young, Ed.), Ch. 13. Oxford Univ. Press, New York, 1993.
15. Y.-I. Kim, and F. Izumi, *J. Ceram. Soc. Jpn.* **102**, 401 (1994).
16. A. C. Larson, and R. B. Von Dreele, "GSAS—General Structure Analysis System," Los Alamos National Laboratory Report LAUR 86-748 1986.
17. B. I. Lazoryak, *Russ. Chem. Rev.* **65**(4), 287 (1996).
18. R. D. Shannon, *Acta Crystallogr. Sect. B* **32**, 751 (1976).